



Cite this: *Phys. Chem. Chem. Phys.*,
2015, 17, 23741

Controlling pyridinic, pyrrolic, graphitic, and molecular nitrogen in multi-wall carbon nanotubes using precursors with different N/C ratios in aerosol assisted chemical vapor deposition

L. G. Bulusheva,^{*ab} A. V. Okotrub,^{ab} Yu. V. Fedoseeva,^{ab} A. G. Kurennya,^a
I. P. Asanov,^{ab} O. Y. Vilkov,^c A. A. Koós^d and N. Grobert^{†d}

Nitrogen-containing multi-wall carbon nanotubes (N-MWCNTs) were synthesized using aerosol assisted chemical vapor deposition (CVD) techniques in conjunction with benzylamine:ferrocene or acetonitrile:ferrocene mixtures. Different amounts of toluene were added to these mixtures in order to change the N/C ratio of the feedstock. X-ray photoelectron and near-edge X-ray absorption fine structure spectroscopy detected pyridinic, pyrrolic, graphitic, and molecular nitrogen forms in the N-MWCNT samples. Analysis of the spectral data indicated that whilst the nature of the nitrogen-containing precursor has little effect on the concentrations of the different forms of nitrogen in N-MWCNTs, the N/C ratio in the feedstock appeared to be the determining factor. When the N/C ratio was lower than ca. 0.01, all four forms existed in equal concentrations, for N/C ratios above 0.01, graphitic and molecular nitrogen were dominant. Furthermore, higher concentrations of pyridinic nitrogen in the outer shells and N₂ molecules in the core of the as-produced N-MWCNTs suggest that the precursors were decomposed into individual atoms, which interacted with the catalyst surface to form CN and NH species or in fact diffused through the bulk of the catalyst particles. These findings are important for a better understanding of possible growth mechanisms for heteroatom-containing carbon nanotubes (CNTs) and therefore paving the way for controlling the spatial distribution of foreign elements in the CNTs using CVD processes.

Received 5th April 2015,
Accepted 15th June 2015

DOI: 10.1039/c5cp01981h

www.rsc.org/pccp

1. Introduction

Incorporation of nitrogen atoms in the walls of carbon nanotubes (CNTs) is an attractive method for tuning their electronic and chemical properties.^{1–3} Particularly, as compared to the pure counterparts, nitrogen-containing double-wall and multi-wall CNTs (N-DWCNTs and N-MWCNTs) exhibit better performance as cold electron emitters,^{4–6} supports for catalyst nanoparticles,^{7–9} electrodes in electrochemical capacitors^{10,11} and Li-ion batteries.^{12,13} Catalytic chemical vapor deposition (CCVD) techniques are well established and widely applied for the generation of N-CNTs. It was shown that the concentration and the type of nitrogen depend on the synthesis temperature, gas flow rate, and nature of the catalyst as well as the type of nitrogen precursor.^{14–17} The most common forms of embedded nitrogen discussed in the

literature are graphitic, pyridinic and pyrrolic nitrogen.^{1,18–20} Graphitic nitrogen refers to a nitrogen atom with three carbon neighbours in a hexagonal lattice, if the nitrogen is two-fold coordinated similar to that is found in pyridine, it is called pyridinic, and three-fold coordinated nitrogen in a region of defective non-aromatic lattice is associated with pyrrolic nitrogen. While the majority of reports argue that, due to their different stabilities, the concentration of these different types of nitrogen atoms in N-MWCNTs is largely controlled by the synthesis temperature^{21,22} some accounts also consider the nature of the precursor to be a crucial factor. For instance, when acetonitrile was mixed with short-chain alcohols, pyridinic nitrogen was not observed in N-MWCNTs.²³ With increasing melamine concentration in the feedstock material, an increase in the ratio of pyridinic to graphitic nitrogen was observed and attributed to the presence of the CN bonds in the precursor contributing to the pyridinic nitrogen formation.²⁴ Jian *et al.* conducted a study using different nitrogen-containing precursors with the aim of controlling the type of nitrogen atoms present in the N-MWCNTs whereby the precursors contained nitrogen atoms in an aromatic ring and/or in an amine group.²⁵ Whilst the investigation revealed a general increase of nitrogen in the

^a Nikolaev Institute of Inorganic Chemistry, SB RAS, 630090 Novosibirsk, Russia.
E-mail: bul@niic.nsc.ru

^b Novosibirsk State University, 630090 Novosibirsk, Russia

^c St. Petersburg State University, 198504 St. Petersburg, Russia

^d Department of Materials, University of Oxford, Oxford OX1 3PH, UK

[†] Present address: Institute for Technical Physics and Materials Science, Konkoly-Thege ut. 29-33, 1121 Budapest, Hungary.

N-MWCNTs product with increasing N/C ratios in the initial precursor, the variation in the forms of the embedded nitrogen atoms was not discussed and most likely because no dependence could be identified. Comparison of the amine and amide precursors for the N-MWCNTs growth showed that the N/C ratio in the feedstock material has a more noticeable effect on the morphology and nanotube yield than the actual nature of the nitrogen source.²⁶

The mechanism of CCVD growth of CNTs is not yet fully understood²⁷ and the question how the type of C–N bonding in the precursor may influence the forms of the incorporated nitrogen remains open. For nanotubes to form, the first step necessary in the synthesis process is the decomposition of a solid, liquid, or gaseous carbon-containing precursor, on a catalytic surface which can be a metal thin film or metal catalyst particles. However, the products of the cracking of the nitrogen-containing precursor molecules are usually unknown.²⁸ It could be atoms, dimers, or stable fragments such as, for example, phenyl. The second step in the growth process includes the diffusion of the cracking products through the bulk of a catalyst, in the subsurface layers, or on the surface of the catalyst particle followed by the extrusion of carbon to form a nanotube.²⁹ Studies using density functional theory (DFT) revealed that atomic carbon and nitrogen possess quite small energy barriers with regard to their mobility on an iron cluster, and tend to interact readily, producing C₂ and CN units.³⁰ Molecular dynamic simulation confirmed that these units move faster on the surface of iron nanoparticles than individual atoms do.³¹ Therefore, the direct dependence between pre-existing CN bonds in the precursor and the predominant form of nitrogen in the N-CNTs can be expected only if the precursor dissociates incompletely and the obtained N-containing species diffuse on the surface of a catalyst particle.

Here, we study the presence of the different forms of nitrogen in N-MWCNTs using precursors containing CN and NH₂ bonds, namely, acetonitrile (CH₃CN) and benzylamine (C₆H₅CH₂NH₂) in conjunction with aerosol assisted CCVD, where ferrocene was used as a catalyst source. Acetonitrile contains a triple CN bond, which could be the source of the pyridinic nitrogen, while NH₂ species in benzylamine may contribute to the graphitic or pyrrolic nitrogen atoms. X-ray photoelectron spectroscopy (XPS) and near-edge X-ray absorption fine structure (NEXAFS) spectroscopy were used to identify the concentration and the electronic state of nitrogen in the N-MWCNTs. The former spectroscopy is surface-sensitive and

the latter one probes the bulk of a nanotube. Combination of these methods allows detection of a change in the distribution of nitrogen forms from the outer layer to the nanotube core.

2. Experimental

Details of the aerosol assisted CVD setup used for the synthesis of N-MWCNTs studied here can be found elsewhere. N-MWCNTs were produced with solutions of 5 wt% ferrocene [Fe(C₅H₅)₂] in benzylamine³² and acetonitrile.³³ The N/C ratio in acetonitrile and benzylamine are 1 : 2 and 1 : 7 respectively. In order to change this ratio, a certain portion (5 : 95, 50 : 50, and 100 : 0) of toluene C₆H₅CH₃ was added to the reaction mixture. When the horizontal tubular reactor reached 800 °C, the precursor solutions were introduced with an Ar flow rate of 0.14 ml min⁻¹ at atmospheric pressure over a period of 30 min. The synthesis temperature and the gas flow rate were kept constant throughout the experiment in order to minimize any possible influence of these parameters on the incorporation of the nitrogen.

The structure of the as-produced N-MWCNT samples was examined by transmission electron microscopy (TEM, Jeol 2010). IR-absorption spectra were recorded using a Fourier transform spectrometer FTS-2000 by pressing the sample with KBr.

XPS and NEXAFS spectra were recorded at the Berliner Elektronenspeicherring für Synchrotronstrahlung (BESSY) using radiation from the Russian–German beamline. XPS spectra were measured at an energy of monochromatized synchrotron radiation equal to 800 eV. NEXAFS spectra near the N K-edge were acquired in the total-electron yield (TEY) mode with the monochromatization of the incident radiation of ~0.17 eV. The spectra were normalized to the primary photon current from a gold-covered grid recorded simultaneously. To study the change in the electronic state of nitrogen in body of the nanotubes, the XPS spectra were recorded on a Phoibos 150 Specs spectrometer using nonmonochromatic Mg K_α (1253.6 eV) excitation. The binding energies were calibrated relative to the C 1s peak at 284.5 eV.

3. Results

TEM analysis confirmed the presence of multi-wall nanotubes in all samples. A change in the nanotube structure was also observed depending on the N/C ratio in the hydrocarbon feedstock and

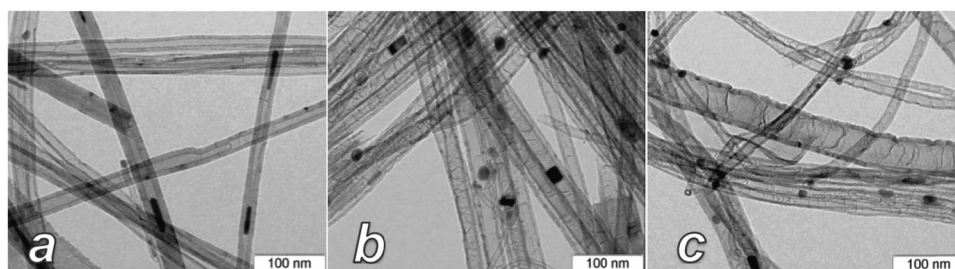


Fig. 1 Transmission electron micrographs of N-MWCNTs synthesized using acetonitrile and toluene mixed in ratios of 5 : 95 (a), 50 : 50 (b), and 100 : 0 (c).

an example of such a change is presented in Fig. 1 showing N-MWCNTs grown from acetonitrile:toluene mixtures of (a) 5:95, (b) 50:50, and (c) 100:0. At the lowest N/C ratio of 1/135 for a precursor ratio of 5:95, the nanotubes exhibit relatively straight and thick walls of ~ 12 nm in average (Fig. 1a). Higher nitrogen concentrations cause a reduction of the number and corrugation of the carbon layers while the diameter of the inner core increases (Fig. 1b and c). Similar structural variation was observed when N-MWCNTs were grown from mixtures of benzylamine/toluene,^{32,34} melamine/ethylene,²⁴ or ammonia/acetylene.³⁵

The nitrogen content in the N-MWCNTs was determined from the ratio of the areas under the C 1s and N 1s peaks taking into consideration the photoionization cross-sections for elements at the given photon energy. The values derived from the survey spectra measured at 800 eV are summarised in Table 1. There is a tendency of enrichment of nitrogen in the nanotubes with higher N/C ratios in the feedstock. N 1s spectra (Fig. 2) revealed the nature of the incorporated nitrogen atoms. Based on the N K-edge NEXAFS spectra, which we will be addressed later, three components located at 398.5, 399.9, and 401.1 eV were

separated in the XPS spectra. With increasing binding energies, the components correspond to pyridinic, pyrrolic, and graphitic nitrogen and we found that the relationship between the N/C ratio in feedstock and the concentration of the respective nitrogen forms incorporated in the N-MWCNTs is ambiguous (Table 1). Our findings show that different forms of nitrogen were present in equal concentrations in both samples, *i.e.* in N-MWCNTs produced with *ca.* 5% benzylamine or 5% acetonitrile. However, with increasing hydrocarbon precursor concentrations the fingerprint of pyrrolic nitrogen in the N 1s spectrum progressively decreases. The components corresponding to the graphitic nitrogen and pyridinic nitrogen have almost equal intensities in the spectra of all investigated N-MWCNTs except for those synthesized from a mixture of acetonitrile:toluene of 50:50 and from benzylamine solely, where the graphitic nitrogen noticeably prevails.

At an excitation energy of 800 eV, the inelastic mean free path of photoelectrons from the N 1s level is estimated to be ~ 1.8 nm.³⁶ Hence, the proportions of different nitrogen forms determined from the XPS spectra fitting (Table 1) correspond to

Table 1 The correlation between the N/C ratio in the hydrocarbon precursors and the total nitrogen content (N_{tot}) and the ratio of pyridinic, pyrrolic, and graphitic nitrogen in the as-produced N-MWCNTs using benzylamine or acetonitrile. The concentration of nitrogen was determined using survey X-ray photoelectron spectra measured at 800 eV

N/C	1/140	1/135	1/14	1/9	1/7	1/2
N-source	$C_7H_7NH_2$	CH_3CN	$C_7H_7NH_2$	CH_3CN	$C_7H_7NH_2$	CH_3CN
N_{tot} (at%)	0.1	0.8	0.4	1.2	1.0	3.0
$N_{\text{pyrid}} : N_{\text{pyrr}} : N_{\text{gr}}$	1 : 1 : 1	1 : 1 : 1	2 : 1 : 2	1.3 : 1 : 2.4	3.4 : 1 : 8	4 : 1 : 4

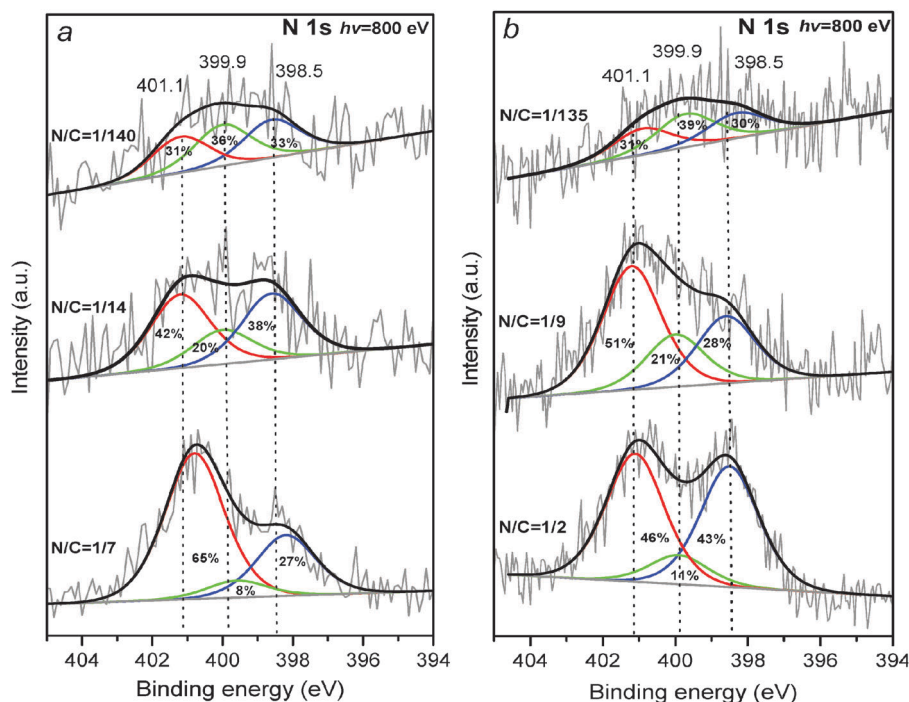


Fig. 2 XPS N 1s spectra of N-MWCNTs synthesized from (a) benzylamine ($N/C = 1/7$) or benzylamine mixed with 50% of toluene ($N/C = 1/14$) and 95% of toluene ($N/C = 1/140$) and (b) acetonitrile ($N/C = 1/2$) or acetonitrile mixed with 50% of toluene ($N/C = 1/9$) and 95% of toluene ($N/C = 1/135$). The spectra were collected at an excitation energy of 800 eV.

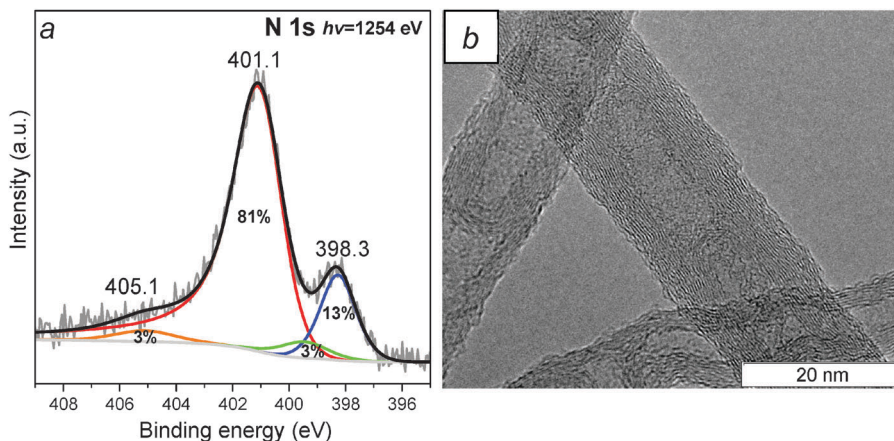


Fig. 3 XPS N 1s spectrum (a) and high-resolution TEM image (b) of N-MWCNTs synthesized from benzylamine. The spectrum was collected at an excitation energy of 1253.6 eV.

about 5 outer layers of the N-MWCNTs. The increase of the photon energy to 1253.6 eV allows registering the photoelectrons from about 7–8 surface layers. The N 1s spectrum measured at this energy for the sample synthesised from benzylamine is shown in Fig. 3. In this particular case, a Doniach-Sunjic high-energy tail with an asymmetry factor³⁷ of 0.04 was added to a Gaussian/Lorentzian product function to describe the main spectral component at ~ 401.1 eV. The asymmetric tail may be related to a satellite arising from the energy loss of electrons associated with the occupied-unoccupied states contributed by nitrogen.³⁸ The N 1s spectrum has a reduced relative area of the component caused by pyridinic nitrogen atoms when compared to the spectrum recorded at 800 eV (Fig. 2a). This implies that pyridinic nitrogen prefers to be in the surface layers. In addition, the spectrum exhibits a component at ~ 405.1 eV assigned to N_2 molecules.³⁹ High-resolution TEM images revealed that the number of layers in the N-MWCNTs is not less than seven. The absence of the signal from the molecular nitrogen in the spectrum recorded at a photon energy of 800 eV and its appearance when the energy was increased to 1253.6 eV indicates that the N_2 molecules are located between the inner layers or in the

nanotube cavity. Scanning transmission X-ray microscopy studies of an individual nitrogen-containing nanotube by Zhou *et al.* revealed the presence of pyridinic and graphitic nitrogen atoms in surface layers and N_2 molecules inside the core of the nanotube.⁴⁰ Our studies on bulk quantities of N-MWCNTs complement these findings.

The average nitrogen content in the sample derived from the XPS data obtained at 1253.6 eV is ~ 1.2 at%, which is higher than that found in the first five nanotube layers (Table 1). Previously, it was shown that N-MWCNTs synthesized from phthalocyanines also showed higher nitrogen levels near the surface rather than in the inner core.⁴¹ In our case, increase in the total nitrogen content is accompanied by a rise of the portions of graphitic and molecular nitrogen.

NEXAFS spectroscopy in the TEY mode registers photoelectrons of depths greater than 10 nm from the surface, thus providing compositional information not only on the nanotube walls but also on probing the nanotube core. Fig. 4 compares the spectra measured near the N K-edge of the synthesized samples. At energies lower than the σ^* edge the spectra show a set of resonances and in the following we firstly focus on the

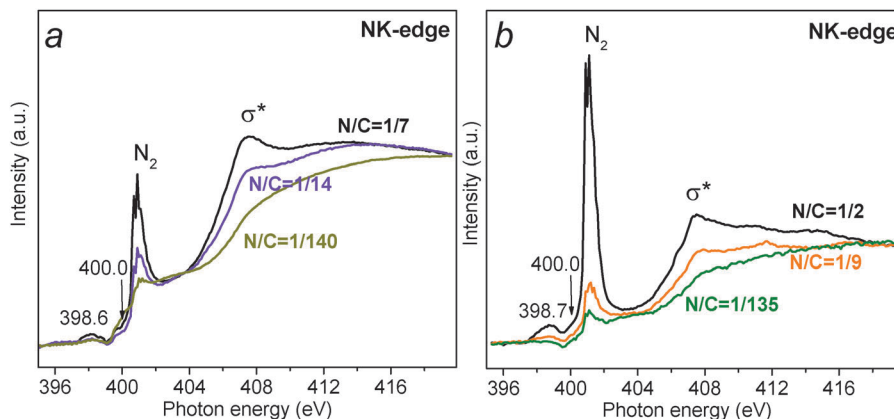


Fig. 4 NEXAFS N K-edge spectra of N-MWCNTs synthesized using (a) benzylamine ($N/C = 1/7$), benzylamine mixed with 50% of toluene ($N/C = 1/14$) or 95% of toluene ($N/C = 1/140$) and (b) acetonitrile ($N/C = 1/2$), acetonitrile mixed with 50% of toluene ($N/C = 1/9$) or 95% of toluene ($N/C = 1/135$).

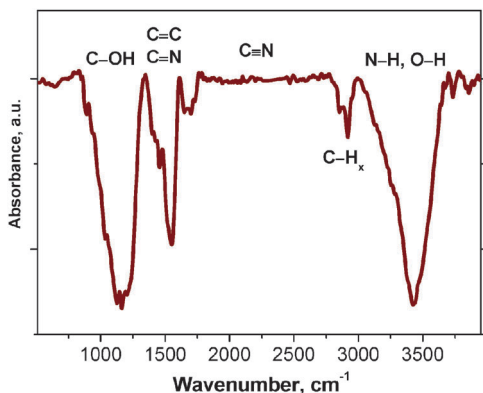


Fig. 5 IR spectrum of N-MWCNTs synthesized from acetonitrile mixed with toluene (50 : 50).

most intense peak. The peak splitting corresponds to the vibrational fine structure of N_2 molecules in N-CNTs.^{42,43} The spectrum of the sample produced from acetonitrile solely exhibits the highest relative intensity of the peak (see Fig. 4b). This intensity progressively decreases with lower nitrogen contents in the feedstock (Fig. 4). The ratio of the heights of the N_2 resonance and σ^* resonance equals ~ 0.67 for an N/C ratio of 1/9 (50% of acetonitrile and 50% of toluene) and ~ 0.82 for the ratio of 1/7 (100% of benzylamine). Interestingly, N_2 molecules are also formed even at very low nitrogen contents in the precursor (1/140 for the mixture of benzylamine and toluene of 5 : 95). Moreover, the N K-edge spectra show a broad resonance of around 398.6–398.7 eV and a resonance at ~ 400.0 eV, which can be attributed to the pyridinic and pyrrolic nitrogen in line with the XPS data. The latter π^* resonance has an energy close to that of the nitril $C\equiv N$ groups.⁴⁴

Although it is difficult imagining how these groups can accommodate between the nanotube layers, we measured the IR-spectrum of the sample produced from the acetonitrile and toluene taken in equal proportions, because the N 1s spectrum of this sample showed a high intensity of the center component of the spectrum (Fig. 2b). The vibration of the triple $C\equiv N$ bond is expected around 2220 cm^{-1} ,⁴⁵ and there the spectrum showed a negligible absorption (Fig. 5). Thus, we suggest that the nitrogen atoms adopt an intermediate state between pyridinic and graphitic nitrogen corresponding to pyrrolic nitrogen atoms. The N–H vibrations around 3200 cm^{-1} are overlapped with the O–H bond vibrations. The resonance related to the $1s \rightarrow \pi^*$ transitions within the graphitic nitrogen should appear at ~ 401.0 eV and in our spectra it is masked by the N_2 resonance. However, this type of nitrogen is responsible for a strong σ^* resonance⁴⁶ thus increasing the relative intensity of the σ^* edge when the amount of trapped N_2 molecules is reduced. Overall, the concentration of all forms of nitrogen decreases with the decrease of the N/C ratio in the feedstock used for the synthesis of N-MWCNTs.

4. Discussion

XPS and NEXAFS analyses of the N-MWCNT samples synthesized by an aerosol assisted CCVD method revealed graphitic,

pyridinic, pyrrolic, and molecular forms of nitrogen. When the concentration of nitrogen in the precursor was low (one nitrogen atom per hundreds of carbon atoms), there was no marked preference of any form. This is a new result; earlier studies using such a low N/C ratio of the reactants have focused on structural configurations of the N-MWCNTs.^{26,32} Increasing the N/C ratio up to an order of magnitude suppressed the formation of pyrrolic nitrogen. Independent of the use of benzylamine or acetonitrile as the precursor, the outer layers of the N-MWCNTs synthesized at $800\text{ }^\circ\text{C}$ contained mainly pyridinic nitrogen while the core stored N_2 gas. Previous studies of N-DWCNTs by Kim *et al.* showed a larger fraction of pyridinic nitrogen in the inner walls⁴⁷ of the nanotubes. This nitrogen form was suggested to release a strain of the curved graphitic sheets better than graphitic nitrogen. In our case, such a strain-releasing effect should be negligible due to the comparatively large diameters of the N-MWCNTs.

The formation of the pyrrolic nitrogen in nanotubes grown from acetonitrile, containing no N–H bonds, evidenced that the precursor was completely decomposed on the surface of the catalytic nanoparticle. The consequent interaction of the nitrogen and hydrogen atoms giving NH species is in accordance with the theoretical considerations of the N-CNT generation.^{30,31} The catalytic cracking of acetonitrile produces more nitrogen atoms as compared to that of benzylamine, and the large fraction of pyridinic nitrogen in the surface layer of nanotubes grown from the acetonitrile solely (Fig. 2b) evidences the high rate recombination of the nitrogen and carbon atoms. The observation that the concentration of pyridinic nitrogen decreases from the surface to the depth of the nanotube, while the concentration of the graphitic nitrogen shows opposite behavior supports the catalytic thermolysis of acetonitrile and benzylamine at $800\text{ }^\circ\text{C}$ down to individual atoms. The atoms should move more easily through the subsurface layers and the bulk of metallic nanoparticle than a bonded combination of atoms, such as a CN pair.

A rise of the N/C ratio in the precursor vapor results in higher concentrations of N_2 trapped in the N-MWCNT core. Since these molecules are in the nanotube cavity or between the inner layers, it is likely that they were generated as a result of nitrogen atoms diffusing through the catalyst particle. Recently, Kamberger *et al.* detected N_2 molecules in single-walled CNTs, produced from an isotope labeled acetonitrile, and explained their existence by the reaction of two $C\equiv N$ radicals at or inside the catalyst particle.⁴⁸ According to NEXAFS and XPS data, this reaction is less likely to occur in N-MWCNTs, but cannot be excluded.

In summary, we illustrate the formation mechanism of N-MWCNTs and the distribution of different forms of nitrogen along the nanotube layers as depicted in Fig. 6a. The shape and location of catalyst nanoparticles were obtained from TEM images and are typical of N-MWCNTs (Fig. 6b). At the catalyst surface, the nitrogen-containing precursor decomposes into atoms. These atoms interact on the surface of the catalyst producing CN and NH species or diffuse through the catalyst nanoparticles. Surface and subsurface diffusion of the CN and NH contribute to the formation of pyridinic and pyrrolic nitrogen mainly in the outer shells of N-MWCNTs. Bulk diffusion of C and N atoms

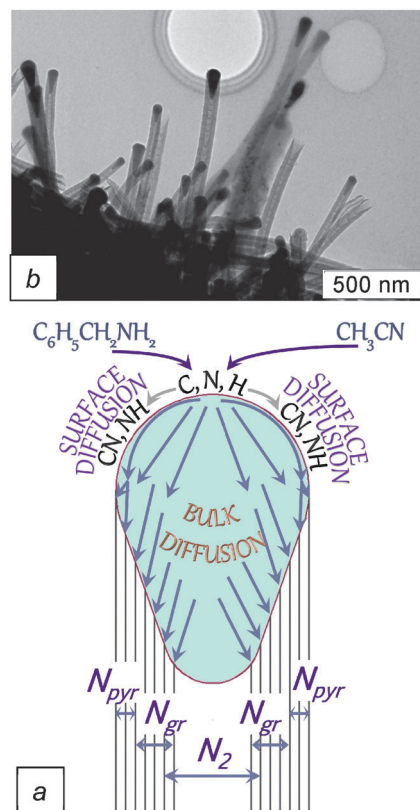


Fig. 6 Schematic diagram of the formation and preferred distribution of different forms of nitrogen (N_{pyr} – pyridinic and pyrrolic, N_{gr} – graphitic) in N-MWCNTs (a). TEM image of the tips of N-MWCNTs synthesized from acetonitrile:toluene of 50:50 (b) served as a basis for the shape and location of catalyst nanoparticle shown in (a).

results in building of the shells enriched with graphitic nitrogen and these shells are closer to the nanotube core. Because graphitic shells can preserve the tubular shape when only a restricted amount of nitrogen atoms are incorporated, the rest of the nitrogen atoms diffusing through the catalyst contribute to the formation of N_2 molecules, which is also confirmed by the Mössbauer spectroscopy study of N-MWCNTs.⁴⁹ The nanotubes, produced under similar conditions as reported here, contained no α -Fe phase, due to the dissolution of nitrogen into the iron catalyst nanoparticles.

5. Conclusion

Different C–N bonding environments may lead to nanotubes with significantly different properties, therefore we comparatively examined N-MWCNTs grown from molecules incorporating significantly different bonds namely acetonitrile CH_3CN and benzylamine $\text{C}_6\text{H}_5\text{CH}_2\text{NH}_2$. We investigated multi-wall carbon nanotubes produced by aerosol assisted CCVD from pure and diluted nitrogen-containing precursors using surface sensitive XPS and bulk probing NEXAFS spectroscopy in order to study and characterize the incorporation and nature of nitrogen atoms within the graphitic network of the MWCNTs. Four chemical forms of nitrogen, namely, pyridinic, pyrrolic, and graphitic

configurations and N_2 molecules were found in the N-MWCNTs independent of the feedstock composition. The analysis of the spectral data revealed no obvious effect of the nature of nitrogen-containing precursor on the probability of the realization of any nitrogen form, while we found the dependence on the N/C ratio in reactants. The increase of the nitrogen content in the feedstock suppresses the incorporation of the pyrrolic nitrogen first and induces the N_2 formation substantially. We suggest that CN and NH species diffuse onto the surface or into subsurface layers of the catalyst nanoparticles, while C and N atoms diffuse into the bulk. Consequently, the properties of N-MWCNTs are independent of the feedstock composition. However, it is possible to tune the incorporation of nitrogen by tuning the N/C ratio of the precursor, and hence their applicability may be extended. Therefore inexpensive nitrogen-containing precursors should in order to reduce the manufacturing costs of N-CNTs. The results obtained are also important for the precise control of the CNT composition through the tuning of the synthesis conditions. Further experiments are envisaged to explore additional experimental parameters to control the N incorporation and reduce the cost of N-MWCNT production.

Acknowledgements

We thank A. V. Ishchenko for the TEM images. This work was supported by the Russian Foundation for Basic Research (grant 13-03-00884-a) and the bilateral Program “Russian-German Laboratory at BESSY” in part of the XPS and NEXAFS measurements. We are also grateful for the financial support received from the European Community’s Seventh Framework Programme (FP7/2007–2013): the Marie Curie CONTACT Project under grant agreement no. 238363; The Royal Society, European Research Council (ERC) Starting Grant (ERC-2009-StG 240500 DEDIGROWTH; and ERC-2012-PoC 309786 DEVICE); UK Government for Engineering and Physical Sciences Research Council (EPSRC) Pathways to Impact grants.

Notes and references

- 1 C. P. Ewels and M. Glerup, *J. Nanosci. Nanotechnol.*, 2005, **5**, 1345.
- 2 P. Ayala, R. Arenal, M. Rummeli, A. Rubio and T. Pichler, *Carbon*, 2010, **48**, 575.
- 3 D. Jana, C.-L. Sun, L.-C. Chen and K.-H. Chen, *Prog. Mater. Sci.*, 2013, **58**, 565.
- 4 K.-Y. Chun, H. S. Lee and C. J. Lee, *Carbon*, 2009, **47**, 169.
- 5 L. G. Bulusheva, O. V. Sedelnikova and A. V. Okotrub, *Int. J. Quantum Chem.*, 2011, **111**, 2696.
- 6 A. Okotrub, A. Kudashov, A. Gusel’nikov and L. Bulusheva, in *Phys., Chem. Appl. Nanostruct.*, ed. V. E. Borisenko, S. V. Gaponenko and V. S. Gurin, Proceedings of the International Conference. Nanomeeting-2007, Minsk, Belarus, 22–25 May 2007, Review and Short Notes, pp. 585–588.
- 7 L. Jia, D. A. Bulusheva, O. Yu. Podyacheva, A. I. Boronin, L. S. Kibis, E. Yu. Gerasimov, S. Beloshapkin, I. A. Seryak, Z. R. Ismagilov and J. R. H. Ross, *J. Catal.*, 2013, **307**, 94.

- 8 X. Lepró, E. Terrés, Y. Vega-Cantú, F. J. Rodríguez-Macías, H. Muramatsu, Y. A. Kim, T. Hayahsi, M. Endo, M. Torres and R. M. Terrones, *Chem. Phys. Lett.*, 2008, **463**, 124.
- 9 L. F. Mabena, S. S. Ray, S. D. Mhlanga and N. J. Coville, *Appl. Nanosci.*, 2011, **1**, 67.
- 10 Y. Zhang, C. Liu, B. Wen, X. Song and T. Li, *Mater. Lett.*, 2011, **65**, 49.
- 11 L. G. Bulusheva, E. O. Fedorovskaya, A. G. Kurennya and A. V. Okotrub, *Phys. Status Solidi B*, 2013, **250**, 2586.
- 12 L. G. Bulusheva, A. V. Okotrub, A. G. Kurennya, H. Zhang, H. Zhang, X. Chen and H. Song, *Carbon*, 2011, **49**, 4013.
- 13 X. Li, J. Liu, Y. Zhang, Y. Li, H. Liu, X. Meng, Y. Yang, D. Geng, D. Wang, R. Li and X. Sun, *J. Power Sources*, 2012, **197**, 238.
- 14 S. van Dommele, A. Romero-Izquierdo, R. Brydson, K. P. de Jong and J. H. Bitter, *Carbon*, 2008, **46**, 138.
- 15 J. Liu, S. Webster and D. L. Carroll, *J. Phys. Chem. B*, 2005, **109**, 15769.
- 16 L. G. Bulusheva, A. V. Okotrub, A. G. Kudashov, E. N. Pazhetnov, A. I. Boronin and D. V. Vyalikh, *Phys. Status Solidi B*, 2007, **244**, 4078.
- 17 E. N. Nxumalo and N. J. Coville, *Materials*, 2010, **3**, 2141.
- 18 T. Sharifi, F. Nitze, H. R. Barzegar, C.-W. Tai, M. Mazurkeiwicz, A. Malolepszy, L. Stobinski and T. Wågberg, *Carbon*, 2012, **50**, 3535.
- 19 M. Scardamaglia, M. Amati, B. Llorente, P. Mudimela, J.-F. Colomer, J. Ghijsen, C. Ewels, R. Snyders, L. Gregoratti and C. Bittencourt, *Carbon*, 2014, **77**, 319.
- 20 T. Susi, T. Pichler and P. Ayala, *Beilstein J. Nanotechnol.*, 2015, **6**, 177.
- 21 K. Chizari, A. Vena, L. Laurentius and U. Sundararaj, *Carbon*, 2014, **68**, 369.
- 22 H. Liu, Y. Zhang, R. Li, X. Sun and H. Abou-Rachid, *J. Nanopart. Res.*, 2012, **14**, 1016.
- 23 G. Bepete, Z. N. Tetana, S. Lindner, M. R. Rümmele, Z. Chiguvare and N. J. Coville, *Carbon*, 2013, **52**, 316.
- 24 H. Liu, Y. Zhang, R. Li, X. Sun, S. Désilets, H. Abou-Rachid, M. Jaidann and L.-S. Lussier, *Carbon*, 2010, **48**, 1490.
- 25 G. Jian, Y. Zhao, Q. Wu, L. Yang, X. Wang and Z. Hu, *J. Phys. Chem. C*, 2013, **117**, 7811.
- 26 E. N. Nxumalo, P. J. Letsoalo, L. M. Cele and N. J. Coville, *J. Organomet. Chem.*, 2010, **695**, 2596.
- 27 K. J. MacKenzie, O. M. Dunens and A. T. Harris, *Ind. Eng. Chem. Res.*, 2010, **49**, 5323.
- 28 S. S. Meysami, A. A. Koós, F. Dillon and N. Grobert, *Carbon*, 2013, **58**, 159.
- 29 V. Jourdain and C. Bichara, *Carbon*, 2013, **58**, 2.
- 30 T. Susi, G. Lanzani, A. G. Nasibulin, P. Ayala, T. Jiang, T. Bligaard, K. Laasonen and E. I. Kauppinen, *Phys. Chem. Chem. Phys.*, 2011, **13**, 11303.
- 31 S. Taubert and K. Laasonen, *J. Phys. Chem.*, 2012, **116**, 18538.
- 32 A. A. Koós, M. Dowling, K. Jurkschat, A. Crossley and N. Grobert, *Carbon*, 2009, **47**, 30.
- 33 A. G. Kudashov, A. G. Kurennya, A. V. Okotrub, A. V. Gusel'nikov, V. S. Danilovich and L. G. Bulusheva, *Tech. Phys.*, 2007, **52**, 1627.
- 34 R. J. Nicholls, Z. Aslam, M. C. Sarahan, A. M. Sanchez, F. Dillon, A. A. Koós, P. D. Nellist and N. Grobert, *Phys. Chem. Chem. Phys.*, 2015, **17**, 2137.
- 35 J. W. Jang, C. E. Lee, S. C. Lyu, T. J. Lee and C. J. Lee, *Appl. Phys. Lett.*, 2004, **84**, 2877.
- 36 M. P. Seah and W. A. Dench, *Surf. Interface Anal.*, 1979, **1**, 2.
- 37 S. Doniach and M. Sunjic, *J. Phys. C: Solid State Phys.*, 1970, **3**, 285.
- 38 J.-P. Savy, D. de Caro, C. Faulmann, L. Valade, M. Almeida, T. Koike, H. Fujiwara, T. Sugimoto, J. Fraxedas, T. Ondarçuhu and C. Pasquier, *New J. Chem.*, 2007, **31**, 519.
- 39 C. Puglia, P. Bennich, J. Hasselström, C. Ribbing, P. A. Brühwiler, A. Nilson, Z. Y. Li and N. Mårtensson, *Surf. Sci.*, 1998, **414**, 118.
- 40 J. Zhou, J. Wang, H. Liu, M. N. Banis, X. Sun and T.-K. Sham, *J. Phys. Chem. Lett.*, 2010, **1**, 1709.
- 41 H. C. Choi, J. Park and B. Kim, *J. Phys. Chem. B*, 2005, **109**, 4333.
- 42 J. H. Yang, D. H. Lee, M. H. Yum, Y. S. Shin, E. J. Kim, C.-Y. Park, M. H. Kwon, C. W. Yang, J.-B. Yoo, H.-J. Song, H.-J. Shin, Y.-W. Jin and J.-M. Kim, *Carbon*, 2006, **44**, 2219.
- 43 A. V. Okotrub, L. G. Bulusheva, A. G. Kudashov, V. V. Belavin, D. V. Vyalikh and S. L. Molodtsov, *Appl. Phys. A: Mater. Sci. Process.*, 2009, **94**, 437.
- 44 A. P. Hitchcock and C. E. Brion, *Chem. Phys.*, 1979, **37**, 319.
- 45 A. Majumdar, S. C. Das, T. Shripathi, J. Heinicke and R. Hipper, *Surf. Sci.*, 2013, **609**, 53.
- 46 L. G. Bulusheva, A. V. Okotrub, A. G. Kudashov, Yu. V. Shubin, E. V. Shlyakhova, N. F. Yudanov, E. M. Pazhetnov, A. I. Boronin and D. V. Vyalikh, *Carbon*, 2008, **46**, 864.
- 47 S. Y. Kim, J. Lee, C. W. Na, J. Park, K. Seo and B. Kim, *Chem. Phys. Lett.*, 2005, **413**, 3000.
- 48 C. Kramberger, T. Thurakitseree, E. Einarsson, A. Takashima, T. Kinoshita, T. Muro and S. Maruyama, *Nanoscale*, 2014, **6**, 1525.
- 49 I. S. Lyubutin, O. A. Anosova, K. V. Frolov, S. N. Sulyanov, A. V. Okotrub, A. G. Kudashov and L. G. Bulusheva, *Carbon*, 2012, **50**, 2628.